RECORDSOF CHEMICAL SCIENCES

Accepted: 11th June, 2025
Published: 29th June, 2025

1. 1Department of Chemistry and Industrial Chemistry, Kwara State University, Malete, Nigeria
2. Department of Microbiology, Kwara State University, Malete, Nigeria.

**Corresponding Author:*
Wahab A. Osunniran
wahab.osunniran@kwasu.edu.ng

FRsCS Vol. 4 No. 2 (2025)
Official Journal of Dept. of Chemistry, Federal University of Dutsin-Ma, Katsina State.
http://rscs.fudutsinma.edu.ng

ISSN (Online): 2705-2362
ISSN (Print): 2705-2354

Green Synthesis of Silver Nanoparticles Using *Chromobacterium violaceum*: Characterization and Enhanced Antimicrobial Activity against Foodborne Pathogens.

*[1]Akeem A. Jimoh, [2]Taiwo A. Ajao, [1]Abdulfatai T. Ajiboye, [1]Samsudeen O. Azeez, [1]Aliu A. Adeleke, and *[1]Wahab A. Osunniran*

https://doi.org/10.33003/frscs-2025-0402/04

Abstract: This study presents the biosynthesis and characterization of nanoparticles assisted by *Chromobacterium violaceum*, and focuses on their role in antimicrobial activities. The isolation and identification of the organism were conducted using standard biochemical assays, while the characterization of the synthesized nanoparticles was performed using Brunauer–Emmett–Teller (BET) analysis, Fourier Transform Infrared (FTIR) analysis, and X-ray diffraction (XRD). Production of AgNP was confirmed by surface plasmon resonance at 420 nm, peaking on day 4, and was optimal at pH 7. The biochemical assays revealed that the isolated organism is oxidase- and catalase-positive, but unable to ferment lactose or sucrose. BET analysis showed a high specific surface area (222.834 m^2/g) and mesoporosity. FTIR spectra identified various functional groups such as hydroxyls, amides, and aromatics. XRD analysis revealed the crystalline face-centered cubic (FCC) structure of pure AgNPs, with characteristic peaks corresponding to (111), (200), (220), and (311) planes. The antimicrobial analysis demonstrated dose-dependent inhibition of *Bacillus cereus* and *Aspergillus flavus*, with variation in susceptibility among other isolates. The irregular responses of *Staphylococcus aureus* and *Aspergillus niger* at higher doses suggest complex interactions due to aggregation or microbial resistance mechanisms. Conclusively, *C. violaceum*-synthesized AgNPs exhibit promising bioactivity, structural integrity, and surface characteristics for future applications.

Keywords: Biosynthesis, Nanoparticles, *C. violaceum*, Characterization, Antimicrobial activity, and Green synthesis

Introduction

Pigments and dyes are among the most widely used additives in various industries, such as paper, textiles, leather, cosmetics, pharmaceuticals, dye-sensitized solar cells, food and beverages, and more. This is because products made with these additives show improved quality, durability, flavor enhancement, and visual appeal. Naturally occurring pigments are preferred over synthetic ones due to their vivid colors and health benefits, such as antimicrobial, antioxidant, and anti-inflammatory properties. Natural pigments have become much more popular in recent decades because of their proven safety, sustainability, and environmental friendliness (Alegbe & Uthman, 2024; Di Salvo et al., 2023). Among the numerous sources of natural pigments, microorganisms offer the most exciting pathway for the production of pigments (Di Salvo et al., 2023). The growth and development of bacteria are not seasonal, and by controlling the growth conditions, strains of bacteria can be produced more effectively. The synthesis of pigments in bacteria is essential for defense against desiccation, extreme temperatures, oxidative stress, and UV radiation (Sajjad et al., 2020; Wang et al., 2024). Also, the consistencies in the potential high yield, rapid growth, and

sustainability of the bacteria pigments has motivated global food industries' adoption. These benefits of bacteria pigments over those derived from plants and animals have led to a growing interest in these pigments (Venil et al., 2020).

There are many uses for bacterial pigments in food processing; they act as alternatives to synthetic colorants in dairy, beverages, confectionery, and baked goods, aligning with consumer trends toward healthier food choices. Additionally, bacterial pigments help stabilize foods due to their antimicrobial properties that extend shelf life. Advances in fermentation technology and genetic engineering have enabled the large-scale production of notable bacterial pigments like carotenoids and anthocyanins. These pigments also contain beneficial functional ingredients that boost their health benefits (Barreto et al., 2023; Sen et al., 2019).

A class of pigment called carotenoids, which is present in bacteria, has anti-oxidant, anti-microbial, anti-oxidative stress, anti-inflammatory, and anti-cancer effects. These essential qualities render them extremely advantageous in functional foods. These crucial characteristics make them highly beneficial in functional foods. These pigments include melanin produced by different bacterial species such as *Pseudomonas aeruginosa* and Streptomyces, prodigiosin from *Serratia marcescens*, phycocyanin from *Cyanobacteria*, canthaxanthin synthesized by *Dietzia*, and *deinoxanthin* produced by the *Deinococcus* bacteria. *Chromobacterium* produces violacein, a purple pigment with antimicrobial, anti-viral, and anti-oxidant qualities that make it a crucial natural ingredient in the food and pharmaceutical industries (Ghanavati & Nasrollahzadeh, 2023; Sharma et al., 2024; Swapnil et al., 2021; Venil et al., 2020).

Microbial synthesis is a novel and sustainable alternative to traditional methods, enabling the production of biocompatible nanoparticles under mild conditions using bacteria, fungi, and algae. This approach is environmentally friendly, cost-effective, and scalable, ensuring the avoidance of the dangerous chemicals and high energy needs of physical and chemical methods (Adeleke et al., 2024; Osman et al., 2024; Rathod et al., 2024). The release of biomolecules that serve as capping and reducing agents and improve the antimicrobial, antioxidant, and catalytic qualities of nanoparticles is one way that microorganisms such as *Pseudomonas, Bacillus*, and *Aspergillus* species contribute to their production (Huq et al., 2022; Singh et al., 2023). These have made microbial synthesis a key technology for sustainable nanomaterial production with the aid of genetic engineering and developments (Singh et al., 2023). Also, optimization of the fermentation process continues to boost the yield and functionality of nanoparticles (Kumar et al., 2019). This technique has found its applications in the biomedical, food, and environmental cleanup sectors (Srinivasan & Rana, 2024).

Methodology

Water sample collection

Well water samples were aseptically collected randomly into 10 pre-sterilized sample bottles from different locations in the morning inside Malete town, Kwara State. Each bottle was sealed, kept in ice packs for preservation, and transferred to Kwara State University's Microbiology Laboratory in Malete. The samples were transported following accepted microbiological practices to maintain their integrity for further examination. This methodology is consistent with best practices for evaluating water quality for accurate findings (Ajao et al., 2020).

Characterization and identification of bacterial isolates

The pour plate technique was employed to characterize and identify the bacterial isolates. A sterile micropipette was used to aseptically transfer a 1 mL aliquot of each well water sample into a sterile Petri dish. The Petri dish was then filled with 20 mL of sterile nutrient agar supplemented with different concentrations of sodium chloride (NaCl) (w/v): 0.5%, 1.0%, 2.0%, 3.0%, 3.5%, and 5.0%. The water sample and nutrient agar were thoroughly mixed with the other ingredients in the dish to ensure uniform distribution. The plates were incubated for 48 hours at 37 ^{0}C to promote bacterial growth after solidification of the mixture (Sanders, 2012).

Multiple biochemical tests, including urease activity, citrate utilization, oxidase, motility, indole, triple sugar iron (TSI), and glucose fermentation tests, were used to identify the isolates. Reference standards and the obtained biochemical profiles were compared in Bergey's Manual of Determinative Bacteriology (Poyil et al., 2022).

Gram staining, morphological traits, and a series of biochemical tests were used to identify the bacterial species *Chromobacterium violaceum*. Gram staining was used in conjunction with evaluating the morphological characteristics to offer initial insights into the type of bacteria.

Synthesis of nanoparticles using bacteria in broth

The process described by (Jimoh et al., 2022) was used as the synthesis method with slight modifications. Nutrient agar was prepared, autoclaved, and allowed to cool to 45 ^{0}C. A loopful of a 24 hr test culture of *Chromobacterium violaceum* was added to the prepared nutrient agar, and it was then incubated for 24 hr at 37 ^{0}C. The culture was centrifuged, and the supernatant was extracted for AgNP synthesis. After the *Chromobacterium violaceum* culture's collected supernatant was poured into a separate conical flask, a 1:3 ratio of aqueous $AgNO_3$ solution with a concentration of 0.001 M was added. The mixture was stirred in a shaker set at 100 rpm and agitated at 37 ^{0}C in a dark cupboard. A 1 mL of the reaction mixture was sampled at regular intervals to monitor the reduction of silver ions in the solution by *Chromobacterium violaceum* using a spectrophotometer configured to measure absorbance at wavelengths between 300 and 600 nm (Vanaraj et al., 2017). AgNPs were produced at this range of wavelengths, and their physical colors were found to change from purple to dark. The extracted

nanoparticles were purified with methanol and gently washed with deionized water. The nanoparticles were centrifuged and then oven-dried at the optimal temperature of 60 ^{0}C (Melkamu & Bitew, 2021).

Antibacterial properties of the AgNPs

The broth culture method, as outlined by (Pawar et al., 2019), was used to assess the produced nanoparticles' antibacterial properties. To inoculate 9 mL of peptone broth, 0.1 mL of locally isolated, multidrug-resistant strains of *Escherichia coli, Bacillus cereus, Staphylococcus aureus, and Pseudomonas aeruginosa* were standardized to a 0.5 McFarland turbidity (roughly 1 × 10^6 CFU/mL) from 18-hour-old broth cultures. 1 mL solution of AgNPs in DMSO was added in different concentrations of 50, 100, and 150 mg/mL of the mixture. There was also a control group that received no AgNPs. For a full day, all samples were incubated at 37°C. Optical density (OD) was measured at 600 nm following incubation, and the formula was used to determine the percentage of bacterial growth inhibition:

$$\% \text{ Growth inhibition} = \frac{\text{A control} - \text{ODtest}}{\text{ODcontrol}} x100 \quad 1$$

Antifungal properties of the AgNPs

The methods described by (Abdelghany et al., 2020; Moreno-Vargas et al., 2023) were used to evaluate the nanoparticles' antifungal activity against a sample of fungal species. The Potato Dextrose Agar (PDA) medium was supplemented with 50, 100, and 150 µg/mL of AgNPs. Cut from 72-hr-old cultures of *Aspergillus flavus, Aspergillus fumigatus*, and *Aspergillus niger,* agar plugs with a diameter of 6 mm were put onto PDA plates that had been infused with AgNPs. Control plates were also made with the same fungal plugs but without AgNPs. For 72 hr, every plate was incubated at 28 ± 2°C. The formula was used to determine the percentage of growth inhibition after the fungal growth diameter (D) was measured in millimeters following incubation:

$$\% \text{ Growth inhibition} = \frac{\text{Dcontrol} - \text{Dtest}}{\text{Dcontrol}} \times 100 \quad 2$$

Results and Discussion

Biochemical tests' characterisation

The organism's aerobic nature and ability to control reactive oxygen species are demonstrated by its oxidase and catalase positivity, as shown in Table 1. The capacity of the microorganism to use citrate as its only carbon source, typically positive, supports metabolic versatility, and positive motility indicates the presence of flagella promotes movement (Barman et al., 2025). The TSI reaction of alkaline over acid (K/A) and glucose fermentation without gas production indicates that the organism ferments glucose but not lactose or sucrose, and no gas or hydrogen sulfide is produced. The strain's limited capacity to metabolize specific nitrogenous compounds is indicated by negative results for urease activity, indole production, lysine decarboxylase, and ornithine decarboxylase (Lehman, 2005). Nonetheless, it exhibits favorable

outcomes for arginine dihydrolase and nitrate reduction, demonstrating its ability to use arginine through deamination pathways and convert nitrate to nitrite (Kurhaluk & Tkaczenko, 2025). The biochemical test results for the organism show that *Chromobacterium violaceum* has a unique metabolic profile

Table 1: Biochemical tests for the microorganism

Biochemical Test	Result
Urease Activity	Negative
Citrate Utilization	Positive (usually)
Oxidase Test	Positive
Motility	Positive
Indole Production	Negative
Triple Sugar Iron (TSI)	Alkaline (K)/Acid (A)
Glucose Fermentation	Positive (no gas)
Catalase	Positive
Nitrate Reduction	Positive
Arginine Dihydrolase	Positive
Lysine Decarboxylase	Negative
Ornithine Decarboxylase	Negative

Characterization of synthesized nanoparticles

The graph shows how *Chromobacterium violaceum* produces silver nanoparticles (AgNPs) through biosynthesis, as measured by absorbance at 420 nm, a wavelength that is indicative of AgNP surface plasmon resonance. A slow decrease is seen after the peak, which could be caused by oxidative degradation, nanoparticle aggregation, or decreased bacterial cell metabolic activity. Maximum nanoparticle formation occurs at day 4, as indicated by the treated sample's absorbance (red curve), Fig. 1 (a), which increases sharply and peaks at about 24 hr. On the other hand, the control sample (blue triangles) exhibits a flat baseline over time, demonstrating that biological activity alone is responsible for the synthesis of nanoparticles. This pattern indicates a time-dependent biosynthesis process, with the best time to harvest AgNPs for stability and yield being 4 days (Dhaka et al., 2023). Also, the was a gradual increase in the formation of the AgNPs until the optimum pH 7, after which a decline was observed as shown in Fig. 1(b).

Brunauer–Emmett–Teller analysis (BET) analysis

Vital surface and textural features of the synthesized AgNPs are revealed by the BET analysis, as depicted in Table 2. A large surface area is shown by the high specific surface area of 222.834 m^2/g, which is beneficial for catalytic and antimicrobial applications because it increases interaction with target molecules or microbes. An effective adsorption or loading of active compounds are supported by the moderately porous structure indicated by the pore volume of 0.125 cm^3/g. The average pore diameter of 2.137 nm and pore width of 6.195 nm are within

the mesoporous range of 2–50 nm; the nanoparticles are said to have well-developed mesoporosity, which promotes surface reactivity and easier diffusion (Galy et al., 2019)

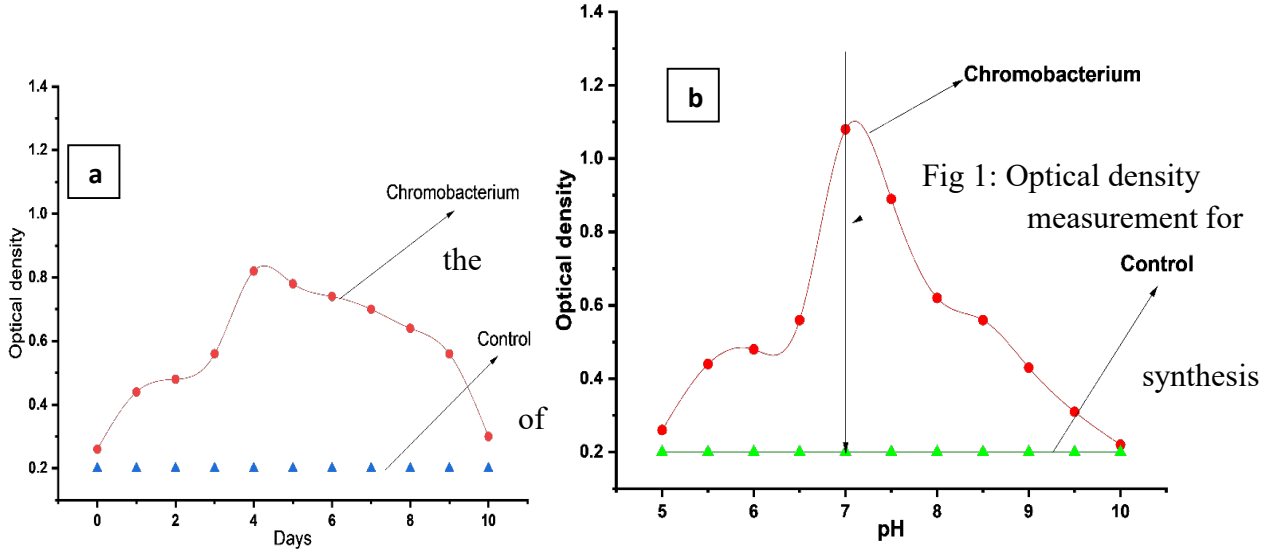

Fig 1: Optical density measurement for the synthesis of nanoparticles (a) versus number of days (b) versus the pH.

These characteristics point to the developed AgNPs' advantageous morphology and porosity profile, which make them appropriate for a range of functional uses, especially in drug delivery, sensing, and antimicrobial activity (Fahim et al., 2024).

Table 2: BET summary

Parameter	Value
BET surface area	222.834 m^3/g
Pore volume	0.125 c^2/g
Pore diameter	2.137 nm
Pore width	6.195 nm

Fourier Transform Infra-red (FTIR) analysis

The FTIR spectrum of the silver nanoparticles (AgNPs) presented in Fig. 2 revealed major absorption peaks. Sharp O–H stretching vibrations peak at 3600 cm^{-1} signify the presence of hydroxyl groups, which could be alcohols or phenolic compounds, and may function as capping agents. The sharp peak at 2200 cm^{-1} is related to C-N stretching from nitriles or C-C stretching from alkynes, suggesting the presence of unsaturated organic molecules involved in stabilizing nanoparticles. A rare peak at 1900 cm^{-1} might result from metal–carbonyl interactions or anhydride (C=O asymmetric stretching), possibly as a result of trace organometallic complexes created during synthesis. The sharp band at 1600 cm^{-1} indicates C=C stretching of aromatic

rings or amide (C=O stretching) vibrations, which could be proteins or polyphenols attached to the surface of the nanoparticle. The 1450 cm-¹ peak represents C–H bending of methyl and methylene groups. Sharp peak at 1100 cm-¹ that is attributed to C–O–C or C–O stretching contributed by alcohols, ethers, or esters, which can be found in natural polymeric coatings. The peak at 650 cm-¹ reflects metal-ligand (Ag–O or Ag–Cl bond vibrations) interactions crucial for stabilizing nanoparticles. These peaks collectively demonstrate how organic molecules contribute to AgNP reduction and capping (Dhaka et al., 2023). The reducing and stabilizing agents used during synthesis are frequently the source of the sharp peaks at respective wavenumbers in the FTIR spectrum of silver nanoparticles (AgNPs), which represent discrete functional groups (Singhal et al., 2024)

.

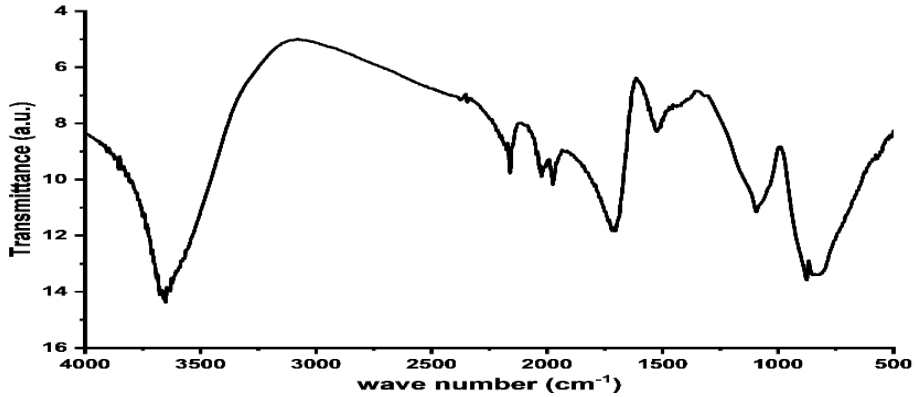

Fig. 2: FTIR spectrum of AgNPs

X-ray diffraction analysis

The XRD result of the AgNPs is presented in Fig. 3, with peaks at 2θ values of 38.8°, 45.6°, 64.8°, and 77.9° as summarised in Table 3, suggesting the formation of a face-centered cubic (FCC) crystalline structure of metallic silver. The peaks are in good agreement with the standard JCPDS card No. and correspond to the (111), (200), (220), and (311) crystal planes respectively. A high degree of crystallinity is indicated by the intensity and sharpness of these peaks, with the (111) plane frequently being the most noticeable, indicating a preferred growth orientation, for pure silver. The AgNPs appear to be phase-pure and lack impurities like silver oxide or silver chloride based on the lack of extra peaks (Hlapisi & Ajibade, 2025). Additionally, the nanoscale size and potential lattice strain within the particles are responsible for any peak broadening. The XRD pattern verifies that pure and highly crystalline silver nanoparticles were successfully synthesized (Ali et al., 2023).

Table 3: X-ray diffraction peak interpretation

2θ (°)	Crystal Plane (hkl)	Phase
38.8°	(111)	FCC
45.6°	(200)	FCC
64.8°	(220)	FCC
77.9°	(311)	FCC

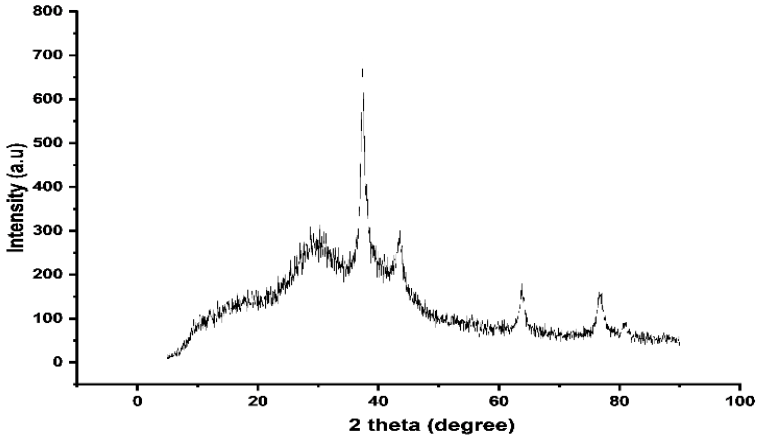

Fig. 3: XRD pattern of the AgNPs

Antimicrobial activities of the AgNPs

The results of the antimicrobial activities are presented in Table 4 and Fig. 4. Antimicrobial efficacy of the AgNPs against selected bacterial and fungal isolates is measured by absorbance optical density (OD) and percentage inhibition. The Effect of the increase in concentration of the AgNPs indicates that the *Bacillus cereus* OD trend decreases (0.420 → 0.297 → 0.269). This showed that AgNPs exhibit potent antibacterial activity that is dose-dependent, suggesting higher efficacy as concentrations increase (Khan et al., 2023). The OD trend for *Staphylococcus aureus* is low at 50 µg/mL (0.278) but rises at 100 and 150 µg/mL. This inverse dose-response could indicate that AgNP aggregation at higher concentrations lowers bioavailability and could activate stress or resistance mechanisms. The trend of *Escherichia coli* OD is decreasing at 100 µg/mL (0.421) and then increasing at 150 µg/mL (0.663). This may have resulted in AgNPs becoming less effective or dispersing inefficiently. *Pseudomonas aeruginosa* OD trend demonstrates very little variation in concentration (0.528–0.555). This showed limited susceptibility or moderate resistance due to the strong outer membrane and efflux systems of *Pseudomonas aeruginosa* (Pang et al., 2019).

The antifungal study indicated that the *Aspergillus fumigatus* OD pattern is slightly increased at 100 g/mL (3.54) but decreased at 150 g/mL (2.75), proposing better

inhibition at the highest dose. The OD pattern of *Aspergillus flavus* decreases consistently (3.03 → 2.67 → 2.53), suggesting that the antifungal activity of AgNPs is dose-dependent and indicating strong antifungal activity at increased doses. However, in *Aspergillus niger*, OD trend sharply dropped at 100 g/mL (2.53), then increases again at 150 g/mL (5.34). This suggests maximum inhibition at 100 g/mL, with reduced efficacy at higher doses, possibly due to clumping or resistance, since AgNPs are broad-spectrum antimicrobials that have species-specific and concentration-dependent effects (Akhter et al., 2024). Among the results, *B. cereus and A. flavus* show the most consistently inhibited species, and the most unexpected dose-resistance patterns are observed in *S. aureus and A. niger*, which warrant further mechanistic studies. AgNP effectiveness may be influenced by particle size and dispersion stability (Mills et al., 2022)

.

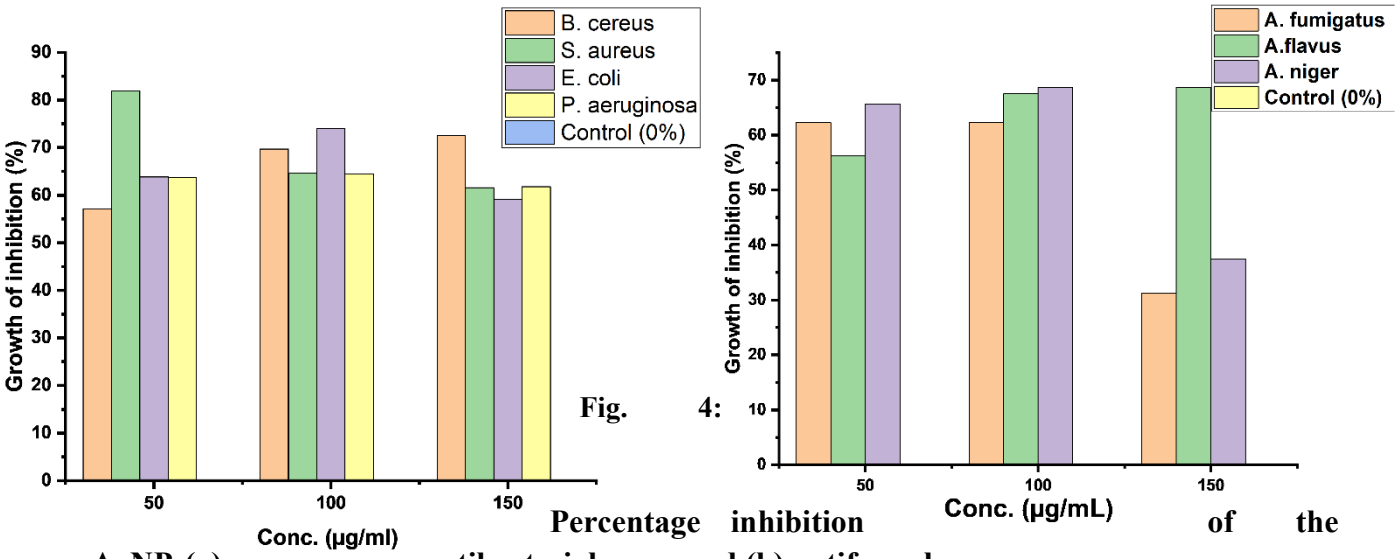

Fig. 4: Percentage inhibition of the AgNPs(a) antibacterial assay and (b) antifungal assay

Table 4. Absorbance of the antibacterial and antifungal assay of the AgNPs

Isolates	Conc. (µg/ml)			
	50 µg/mL	100 µg/mL	150 µg/mL	Control
B. cereus	0.420±0.04	0.297±0.03	0.269±0.01	0.982
S. aureus	0.278±0.01	0.551±0.01	0.591±0.04	1.538
E. coli	0.585±0.03	0.421±0.02	0.663±0.11	1.622
P. aeruginosa	0.528±0.09	0.517±0.07	0.555±0.11	1.455
A. fumigatus	3.02±0.24	3.54±0.35	2.75±0.24	8
A. flavus	3.03±0.26	2.67±0.24	2.53±0.22	8
A. niger	5.55±0.59	2.53±0.17	5.34±0.54	8

Conclusion

The biosynthesis of AgNPs assisted by *Chromobacterium violaceum* was successfully achieved through a green method using biological agents in the organism. The biosynthesized AgNPs display favorable physicochemical properties, such as high surface area, mesoporosity, and crystallinity, which contribute to enhanced bio-interactivity and antimicrobial applications. Spectroscopic and diffraction analyses reveal the presence of organic compounds and pure crystalline phases essential for nanoparticle stability and effectiveness. The results of the antimicrobial tests show strong activity against bacterial and fungal pathogens, especially *Bacillus cereus* and *Aspergillus flavus*, although this activity varies depending on the species and concentration. Differences in dose response among some isolates indicate the need for further research into resistance mechanisms, nanoparticle aggregation, and bioavailability. These findings position C. violaceum-derived AgNPs as promising candidates for eco-friendly, biologically produced nanomaterials in antimicrobial, food industry, and pharmaceutical applications.

Acknowledgement: The authors wish to acknowledge the financial support from the Tertiary Education Trust Fund (TETFUND).

References

Abdelghany, T. M., Hassan, M. M., & El-Naggar, M. A. (2020). GC/MS analysis of Juniperus procera extract and its activity with silver nanoparticles against Aspergillus flavus growth and aflatoxins production. *Biotechnology Reports*, *27*, 1–8. https://doi.org/10.1016/j.btre.2020.e00496

Adeleke, B. S., Olowe, O. M., Ayilara, M. S., Fasusi, O. A., Omotayo, O. P., Fadiji, A. E., Onwudiwe, D. C., & Babalola, O. O. (2024). Biosynthesis of nanoparticles using microorganisms: A focus on endophytic fungi. *Heliyon*, *10*(21), 1–19. https://doi.org/10.1016/j.heliyon.2024.e39636

Ajao, T. A., Oluwatosin, A. N., & Olamide, B. (2020). Bacteriological Surveillance and Assessment of Malete Well Water in Malete , Kwara State. *CITS*, *3*(1), 33–39.

Akhter, M. S., Rahman, M. A., Ripon, R. K., Mubarak, M., Akter, M., Mahbub, S., Al Mamun, F., & Sikder, M. T. (2024). A systematic review on green synthesis of silver nanoparticles using plants extract and their bio-medical applications. *Heliyon*, *10*(11), 1–39. https://doi.org/10.1016/j.heliyon.2024.e29766

Alegbe, E. O., & Uthman, T. O. (2024). A review of history, properties, classification, applications and challenges of natural and synthetic dyes. *Heliyon*, *10*(13), 1–19. https://doi.org/10.1016/j.heliyon.2024.e33646

Ali, M. H., Azad, M. A. K., Khan, K. A., Rahman, M. O., Chakma, U., & Kumer, A. (2023). Analysis of Crystallographic Structures and Properties of Silver Nanoparticles Synthesized Using PKL Extract and

Nanoscale Characterization Techniques. *ACS Omega*, *8*(31), 1–10. https://doi.org/10.1021/acsomega.3c01261

Barman, P., Sinha, S., & Chakraborty, R. (2025). Leclercia barmai sp. nov., isolated from worm castings of Eisenia fetida, is a urease-positive, 3-nitropropionic acid and glycerol-consuming bacterium. *Scientific Reports*, *15*(1), 1–11. https://doi.org/10.1038/s41598-024-78134-7

Barreto, J. V. de O., Casanova, L. M., Junior, A. N., Reis-Mansur, M. C. P. P., & Vermelho, A. B. (2023). Microbial Pigments: Major Groups and Industrial Applications. *Microorganisms*, *11*(12), 1–38. https://doi.org/10.3390/microorganisms11122920

Dhaka, A., Chand Mali, S., Sharma, S., & Trivedi, R. (2023). A review on biological synthesis of silver nanoparticles and their potential applications. *Results in Chemistry*, *6*(March), 1–23. https://doi.org/10.1016/j.rechem.2023.101108

Di Salvo, E., Lo Vecchio, G., De Pasquale, R., De Maria, L., Tardugno, R., Vadalà, R., & Cicero, N. (2023). Natural Pigments Production and Their Application in Food, Health and Other Industries. *Nutrients*, *15*(8), 1–27. https://doi.org/10.3390/nu15081923

Fahim, M., Shahzaib, A., Nishat, N., Jahan, A., Bhat, T. A., & Inam, A. (2024). Green synthesis of silver nanoparticles: A comprehensive review of methods, influencing factors, and applications. *JCIS Open*, *16*(September), 1–23. https://doi.org/10.1016/j.jciso.2024.100125

Galy, T., Mu, D., Marszewski, M., & Pilon, L. (2019). Computer-generated mesoporous materials and associated structural characterization. *Computational Materials Science*, *157*, 156–167. https://doi.org/10.1016/j.commatsci.2018.10.035

Ghanavati, M., & Nasrollahzadeh, J. (2023). A calorie-restricted diet enriched with tree nuts and peanuts reduces the expression of CX3CR1 in peripheral blood mononuclear cells in patients with coronary artery disease. *International Journal for Vitamin and Nutrition Research*, *93*(4), 329–338. https://doi.org/10.1024/0300-9831/a000738

Hlapisi, N., & Ajibade, P. A. (2025). Preparation of pure phase silver nanoparticles: Morphological, optical, binding interactions with bovine serum albumin and antioxidant potential studies. *Journal of Molecular Structure*, *1322*(P1), 1–11. https://doi.org/10.1016/j.molstruc.2024.140219

Huq, A., Rahman, M. M., & Balusamy, S. R. (2022). Green Synthesis and Potential Antibacterial Applications of. *Polymers*, *742*, 1–22.

Jimoh, A. ., Akpeji, B. ., Azeez, S. ., Ayipo, Y. ., Abdulsalam, Z. ., Adebayo, Z. ., Ajao, A. ., Zakariyah, A. ., & Elemike, E. . (2022). Biosynthesis of Ag and TiO2 nanoparticles and the evaluation

of their antibacterial activities. *Inorganic Chemistry Communications*, *141*, 1–8. https://doi.org/10.1016/J.INOCHE.2022.109503

Khan, S., Rukayadi, Y., Jaafar, A. H., & Ahmad, N. H. (2023). Antibacterial potential of silver nanoparticles (SP-AgNPs) synthesized from Syzygium polyanthum (Wight) Walp. against selected foodborne pathogens. *Heliyon*, *9*(12), 1–12. https://doi.org/10.1016/j.heliyon.2023.e22771

Kumar, G., Mathimani, T., Rene, E. R., & Pugazhendhi, A. (2019). ScienceDirect Application of nanotechnology in dark fermentation for enhanced biohydrogen production using inorganic nanoparticles. *International Journal of Hydrogen Energy*, *4*, 1–7.

Kurhaluk, N., & Tkaczenko, H. (2025). L-Arginine and Nitric Oxide in Vascular Regulation—Experimental Findings in the Context of Blood Donation. *Nutrients* , *17*(4), 1–43. https://doi.org/10.3390/nu17040665

Lehman, D. (2005). Triple Sugar Iron Test Protocols. *American Society for Microbiology*, *September 2005*, 2–3. https://legacy.bd.com/europe/regulatory/Assets/IFU/HB/CE/PA/ES-PA-254458.pdf

Melkamu, W. W., & Bitew, L. T. (2021). Green synthesis of silver nanoparticles using Hagenia abyssinica (Bruce) J.F. Gmel plant leaf extract and their antibacterial and anti-oxidant activities. *Heliyon*, *7*(11), 1–11. https://doi.org/10.1016/j.heliyon.2021.e08459

Mills, E., Sullivan, E., & Kovac, J. (2022). Comparative Analysis of Bacillus cereus Group Isolates' Resistance Using Disk Diffusion and Broth Microdilution and the Correlation between Antimicrobial Resistance Phenotypes and Genotypes. *Applied and Environmental Microbiology*, *88*(6), 1–14. https://doi.org/10.1128/aem.02302-21

Moreno-Vargas, J. M., Echeverry-Cardona, L. M., Moreno-Montoya, L. E., & Restrepo-Parra, E. (2023). Evaluation of Antifungal Activity of Ag Nanoparticles Synthetized by Green Chemistry against Fusarium solani and Rhizopus stolonifera. *Nanomaterials*, *13*(3), 1–15. https://doi.org/10.3390/nano13030548

Osman, A. I., Zhang, Y., Farghali, M., Rashwan, A. K., Eltaweil, A. S., Abd El-Monaem, E. M., Mohamed, I. M. A., Badr, M. M., Ihara, I., Rooney, D. W., & Yap, P. S. (2024). Synthesis of green nanoparticles for energy, biomedical, environmental, agricultural, and food applications: A review. In *Environmental Chemistry Letters* (Vol. 22, Issue 2). Springer International Publishing. https://doi.org/10.1007/s10311-023-01682-3

Pang, Z., Raudonis, R., Glick, B. R., Lin, T. J., & Cheng, Z. (2019). Antibiotic resistance in Pseudomonas aeruginosa: mechanisms and alternative therapeutic strategies. *Biotechnology Advances*, *37*(1), 177–192. https://doi.org/10.1016/j.biotechadv.20

18.11.013

Pawar, J., Henry, R., Viswanathan, P., Patwardhan, A., & Singh, E. A. (2019). Testing of antibacterial efficacy of CuO nanoparticles by methylene blue reduction test against Bacillus cereus responsible for food spoilage and poisoning. *Indian Chemical Engineer*, *61*(3), 248–253. https://doi.org/10.1080/00194506.2018.1548948

Poyil, M. M., Karuppiah, P., Raja, S. S. S., & Sasikumar, P. (2022). Isolation, Extraction, and Characterization of Verotoxin-producing Escherichia coli O157:H7 from Diarrheal Stool Samples. *Sudan Journal of Medical Sciences*, *17*(1), 116–127. https://doi.org/10.18502/sjms.v17i1.10689

Rathod, S., Preetam, S., Pandey, C., & Bera, S. P. (2024). Exploring synthesis and applications of green nanoparticles and the role of nanotechnology in wastewater treatment. *Biotechnology Reports*, *41*(January), 1–10. https://doi.org/10.1016/j.btre.2024.e00830

Sajjad, W., Din, G., Rafiq, M., Iqbal, A., Khan, S., Zada, S., Ali, B., & Kang, S. (2020). Pigment production by cold-adapted bacteria and fungi: colorful tale of cryosphere with wide range of applications. *Extremophiles*, *24*(4), 447–473. https://doi.org/10.1007/s00792-020-01180-2

Sanders, E. R. (2012). Aseptic laboratory techniques: Plating methods. *Journal of Visualized Experiments*, *63*, 1–18. https://doi.org/10.3791/3064

Sen, T., Barrow, C. J., & Deshmukh, S. K. (2019). Microbial pigments in the food industry—challenges and the way forward. *Frontiers in Nutrition*, *6*(March), 1–14. https://doi.org/10.3389/fnut.2019.00007

Sharma, C., Kamle, M., & Kumar, P. (2024). Microbial-Derived Carotenoids and Their Health Benefits. *Microbiology Research*, *15*(3), 1670–1689. https://doi.org/10.3390/microbiolres15030111

Singh, A. N., Narang, J., Garg, D., Jain, V., Payasi, D., Suleman, S., & Kant, R. (2023). Plant Nano Biology Nanoparticles synthesis via microorganisms and their prospective applications in agriculture ☆. *Plant Nano Biology*, *5*(September), 1–12. https://doi.org/10.1016/j.plana.2023.100047

Singhal, M., Loveleen, L., Manchanda, R., Syed, A., Bahkali, A. H., Wong, L. S., Nimesh, S., & Gupta, N. (2024). Design, synthesis and optimization of silver nanoparticles using Azadirachta indica bark extract and its antibacterial application. *Journal of Agriculture and Food Research*, *16*(October 2023), 1–13. https://doi.org/10.1016/j.jafr.2024.101088

Srinivasan, L. V, & Rana, S. S. (2024). A critical review of various synthesis methods of nanoparticles and their applications in biomedical , regenerative medicine , food packaging

, and environment. *Discover Applied Sciences*, *6*(371), 1–23. https://doi.org/10.1007/s42452-024-06040-8

Swapnil, P., Meena, M., Singh, S. K., Dhuldhaj, U. P., Harish, & Marwal, A. (2021). Vital roles of carotenoids in plants and humans to deteriorate stress with its structure, biosynthesis, metabolic engineering and functional aspects. *Current Plant Biology*, *26*(August 2020), 1–11. https://doi.org/10.1016/j.cpb.2021.100203

Vanaraj, S., Keerthana, B. B., & Preethi, K. (2017). Biosynthesis, Characterization of Silver Nanoparticles Using Quercetin from Clitoria ternatea L to Enhance Toxicity Against Bacterial Biofilm. *Journal of Inorganic and Organometallic Polymers and Materials*, *27*(5), 1412–1422. https://doi.org/10.1007/s10904-017-0595-8

Venil, C. K., Dufossé, L., & Renuka Devi, P. (2020). Bacterial Pigments: Sustainable Compounds With Market Potential for Pharma and Food Industry. *Frontiers in Sustainable Food Systems*, *4*(July), 1–17. https://doi.org/10.3389/fsufs.2020.00100

Wang, Y., Liu, J., Yi, Y., Zhu, L., Liu, M., Zhang, Z., Xie, Q., & Jiang, L. (2024). Insights into the synthesis, engineering, and functions of microbial pigments in Deinococcus bacteria. *Frontiers in Microbiology*, *15*(July), 1–12. https://doi.org/10.3389/fmicb.2024.1447785